Evidence in Support of Levitation Effect as the Reason for Size Dependence of Ionic Conductivity in Water: A Molecular Dynamics Simulation

Pradip Kr. Ghorai[†] **and S. Yashonath***[,†,‡,§]

Solid State and Structural Chemistry Unit, and Center for Condensed Matter Theory, Indian Institute of Science, Bangalore-560012, India

Received: March 12, 2006; In Final Form: April 21, 2006

We report extensive molecular dynamics simulations of (i) model ions in water at high concentrations as a function of the size and charge of the ion as well as (ii) realistic simulation of Cl^- and Br^- ions at low concentrations in water at room temperature. We also analyze existing experimental data in light of the results obtained here. The halide ion simulations have been carried out using the interaction potentials of Koneshan et al. (*J. Phys. Chem. B* **1998**, *102*, 4193). We compute structural and dynamical properties of ions in water and explore their variation with size and charge of the ion. We find that ions of certain intermediate sizes exhibit a maximum in self-diffusivity in agreement with previous experimental measurements and computer simulations. We analyze molecular dynamics trajectories in light of the previous understanding of the levitation effect (LE) and the recent suggestion that ionic conductivity has its origin in LE (*J. Phys. Chem. B* **2005**, *109*, 8120). We report the distribution of void and neck radii that exist amidst water. Our analysis suggests that the ion with maximum self-diffusivity is characterized by a lower activation energy and a single-exponential decay of $F_s(k,t)$. The behavior of these and other related quantities of the ion with maximum self-diffusivity are characteristic of the anomalous regime of the LE. The simulation results of Br^- and Cl^- ions in water also yield results in agreement with the predictions of LE. A plot of experimental conductivity data in the literature for alkali ions in water by Kay and Evans (*J. Phys. Chem.* **1966**, *70*, 2325) also yields a lower activation energy for the ion with maximum conductivity in excellent agreement with the LE. To the best of our knowledge, none of the existing theories predict a lower activation energy for the ion with maximum conductivity.

1. Introduction

One of the perplexing behaviors is the maximum in ionic coductivity in polar solvents as the size of the ion increases. Such a maximum has been seen in polar solvents such as water, methanol, acetonitrile, and so forth. Alkali ions as well as halide ions show a maximum in conductivity suggesting that such a maximum exists irrespective of the sign of the charge on the ion. Solvents with hydrogen bonds such as water, methanol, ethanol, and so forth, as well as a number of non-hydrogen bonded solvents such as acetonitrile and pyridine are seen to exhibit such a maximum.[1−4] This maximum in conductivity arises from a similar maximum in mobility of the ion or self-diffusivity. Thus, this maximum in conductivity is a universal behavior of ions in polar solvents.

Ionic conductivity is one of the most accurately measurable quantities. As a result, there exists a large amount of data in the literature. Water is one of the well-known solvents and plays an important role in many chemical as well as biological processes. The existence of the conductivity maximum has been most widely studied in water as compared with any other solvent.[5] The availability of measured conductivity data is useful, especially to verify the predictions of theories or calculations. Fortunately, the existence of reasonably accurate potentials to model water, as well as interactions between water and the ion, has led to the availability of results from realistic simulations.

Starting with Born,[6] a number of groups have investigated the maximum in ionic conductivity in polar solvents. These are aimed at providing a reasonable theoretical framework to understand the underlying cause for the observed size-dependent maximum in ionic conductivity. An early attempt is the solvent−berg model. It suggests that smaller ions have higher charge density and therefore are strongly interacting with the nearest-neighbor shell of solvent molecules.[7] The ion essentially carries this shell of solvent molecules long enough that this leads to a larger effective diameter which lowers its conductivity to a value smaller than the conductivity of larger ions which lack such a strongly interacting solvent shell.

Another set of theoretical attempts to reproduce the observed conductivity (Λ) variation with ion radius is based on continuum models. Here, friction arising from the polarization interaction between the ion field and the solvent is included along with the hydrodynamic friction arising from the viscosity of the solvent η. Born, Fuoss, Boyd, Zwanzig, and Hubbard and Onsager[6−11] attempted to explain the observed maximum in terms of the slow relaxation of the dielectric medium (solvent), induced by the electric field of the ion as the ion diffuses. This gives rise to the dielectric friction, ζ_{DF}, which is given by the expression due to Zwanzig[10,12]

$$\zeta_{DF} = 3q_i^2(\epsilon_0 - \epsilon_\infty)\tau_D/(cr_i^3(2\epsilon_0 + 1)\epsilon_0) \qquad (1)$$

* To whom correspondence should be addressed. E-mail: yashonath@sscu.iisc.ernet.in.
† Solid State and Structural Chemistry Unit.
‡ Center for Condensed Matter.
§ Also at the Jawaharlal Nehru Centre for Advanced Scientific Research, Jakkur, Bangalore.

10.1021/jp061511w CCC: $33.50
Published on Web 06/02/2006

where τ_D is the dielectric relaxation time of the solvent associated with the dynamical properties in continuum treatments and ϵ_0 and ϵ_∞ are the static and high-frequency dielectric constants of the solvent. r_i and q_i are the radius and charge of the ion. The friction due to shear viscosity of the solvent, the hydrodynamic friction (which may arise from short-range interactions), is given by Stokes law

$$\zeta_{SR} = c\pi\eta r_i \tag{2}$$

In the above expressions, the value of c depends on the hydrodynamic boundary condition and equals 4 for the slip boundary condition. Thus, the total friction on the ion, ζ, is

$$\zeta = \zeta_{SR} + \zeta_{DF} \tag{3}$$

Note that while ζ_{SR} is higher, the larger the size of the ion, ζ_{DF} has a $1/r_i^3$ dependence and is higher for ions with smaller radius. The result is that at some intermediate size of the ion, r_i, the total friction ζ is lowest when both terms ζ_{SR} and ζ_{DF} are not too large. This explains the conductivity maximum observed experimentally. Hubbard and Onsager have improved this treatment which leads to better agreement with experimental mobilities.

Although the maximum in ionic conductivity can be reproduced by the continuum treatment for ions carrying a given type of charge-positive or negative-the theory does not permit distinction between them as ζ_{DF} depends on q_i^2. Thus, the theory cannot account for the two different curves in the plot of limiting ion conductivity, $\Lambda_0 - 1/r_i$, obtained experimentally for positive and negative ions and two different maxima.[13]

To overcome the deficiencies of the continuum theories, Wolynes proposed a molecular theory in which he separated the contribution into those from the hard repulsive interaction ζ_{HH} and soft attractive interaction ζ_{SS}. Thus, the friction has been separated into terms arising from the soft attractive forces and the hard repulsive forces. The correlations between the soft and hard interactions are neglected. ζ_{HH} is identified with the hydrodynamic friction. Both solvent−berg and continuum treatments are found as limiting cases of this molecular theory.

Bagchi and co-workers[14−17] have extended the molecular theory to permit self-motion of the ion. This provides a clearer picture of the various physical factors responsible for the friction on the moving ion. These are based on the mode coupling theory and separate the overall friction into a microscopic ζ_{micro} and a hydrodynamic part ζ_{hyd}

$$\frac{1}{\zeta} = \frac{1}{\zeta_{micro}} + \frac{1}{\zeta_{hyd}} \tag{4}$$

ζ_{micro} has contributions from several terms which are discussed by Bagchi and co-workers. Direct binary collisions as well as the isotropic fluctuations in density lead to friction that is represented, respectively, by ζ_{binary} and $\zeta_{density}$. Coupling of the ionic field with polarization fluctuations is responsible for the dielectric friction ζ_{DF}. Thus

$$\zeta_{micro} = \zeta_{binary} + \zeta_{density} + \zeta_{DF} \tag{5}$$

ζ_{hyd} is the so-called hydrodynamic friction. It can be usually determined from transverse current−current correlation function. Although all these terms determine the overall friction on the ion, often some of these terms are less important than others. Thus, for some ions, some of these terms can be neglected. More recent studies by Bagchi and co-workers have shown the importance of ultrafast solvation and that it leads to a significant reduction in the contribution to friction on the ion.[18−22]

Fleming and co-workers,[23] Barbara and co-workers,[24] and Bagchi and co-workers[25] have shown the relationship between the solvation energy time correlation function and the dielectric friction. They have shown that both ion solvation dynamics and dielectric friction are influenced by the dynamics of the ion and the solvent. In other words, the dynamics that influences the ion solvation dynamics is also responsible for the dielectric friction. They show that inclusion of the ultrafast mode in the dielectric relaxation is necessary to obtain closer agreement with the experimentally measured limiting ion conductivity Λ_0.

In the past fifteen years, there have been computer simulation studies which have investigated diffusion of ions in water and other solvents.[26−29] Computer simulations of Rasaiah, Lynden-Bell, and co-workers[26,27] on ion motion in water have clarified some aspects of this intriguing problem. They derived ion−water intermolecular potentials by fitting them to solvation energies of ions in embedded water clusters. They have studied the dependence of mobility on ion radius as well as charge on the ion. Their studies reveal that both positively and negatively charged ions exhibit maximum in mobility. This is consistent with the well-known experimental result on alkali and halide ions which also show a similar maximum. The precise size of the ion at which the maximum in mobility is seen depends on the charge on the ion. Their calculations suggest that the dielectric friction model is more appropriate for larger ions while for small ions the solvent−berg model may be more appropriate. They obtained good agreement with experimental results. More recently, Chandra and co-workers[28] have studied the effect of ion concentration on the hydrogen bond dynamics. They find that water molecules with five hydrogen bonds are more mobile as compared with four or fewer hydrogen bonds.[29,30] They have studied the effect of pressure on aqueous and nonaqueous solutions. They have also reported results of detailed molecular dynamics simulations on ions in water and methanol and water−DMSO mixtures, as a function of ion radius, temperature, and composition.

Experimental studies of ionic mobility in water, alcohols, acetonitrile, and formamide have shown the existence of a maximum in Walden's product.[31−36] Investigations in D_2O show that the ratio of $\Lambda_0\eta_0$ in D_2O to that in H_2O also exhibits a maximum when plotted against r_{ion}^{-1}. Here, Λ_0 is the limiting ion conductivity and η_0 is the viscosity of the solvent. Ionic mobility of cations has also been studied in a series of monohydroxy alcohols.[31,33] It is generally observed that the mobility is lower in these alcohols than that found in water. The mobility is further lowered in higher alcohols. Studies of ionic mobility also exist in solvents such as acetonitrile and formamide.[31,33,36] Both of these solvents exhibit ultrafast solvation dynamics. For acetonitrile, an inertial component with a relaxation time of 70 fs and for formamide around 100 fs have been reported.[37]

Computer simulation studies discussed above of ion conductivity in polar solvents have all been carried out at dilute concentrations to enable comparison with limiting ion conductivities that are usually obtained from experimental data. However, the concentrations at which these calculations have been reported are still far higher than those at which the conductivity is measured experimentally. Experimental measurements are usually made at millimolar concentrations whereas the calculations have been generally carried out at concentrations close to 0.1 M. Further, experiments measure conductivity at several concentrations and extrapolate to zero concentration by

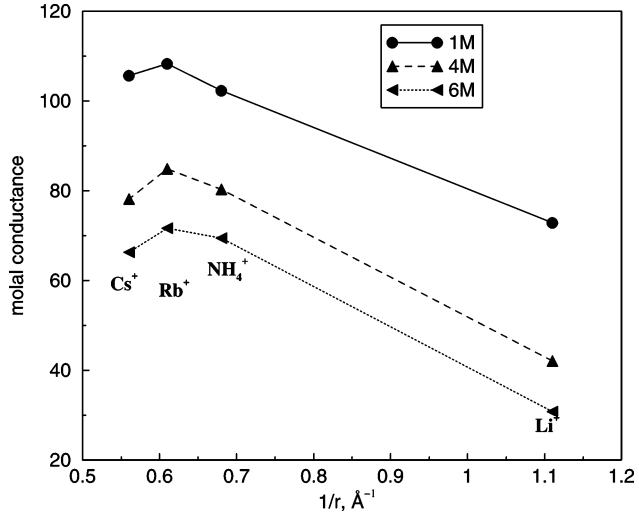

Figure 1. Dependence of conductivity on the size of the ion for different concentrations of solution for LiCl, NH_4Cl, RbCl, and CsCl salts in water at 25 °C at 1, 4, and 6 M (data taken from Goldsack et al.[38]). Note that the position or height of the conductivity maximum remains unchanged with an increase in concentration demonstrating that the nature of the size-dependent conductivity maximum is essentially independent of ionic concentration.

fitting to Kohlrauch's law or a modified form of it to get the limiting ion conductivity, Λ_0.

Calculations performed at lower concentrations are time-consuming and provide poor statistics due to the use of a single ion or a single ion pair. Further, much of the computational effort is spent on solvent molecules since there will be a large number of these. For this reason, it is preferable to carry out simulations at higher concentrations. However, it is not clear whether the size-dependent maximum in ionic conductivity exists at higher ion concentrations. We found that most experiments have been carried out at dilute concentrations. The work of Goldsack et al.,[38] however, report conductivity of a number of chloride and bromide salts in water at 25 °C up to very high concentrations (up to 9 M). In Figure 1, we show the variation of conductivity of LiCl, NH_4Cl, RbCl, and CsCl solutions for different concentrations (1, 4, and 6 M). It is evident from the figure that the size-dependent maximum in ionic conductivity exists even at high concentration (up to 9 M). More importantly, the position at which the maximum is seen as well as the height of the conductivity maximum is seen to be unaltered with an increase in concentration. Although all the ions may not contribute to the ionic conductivity at higher concentrations due to the formation of ion pairs, and so forth, it is seen that this only leads to a decrease in ionic conductivity for *all* sizes of the ion. These measurements of Goldsack et al. suggest that the size-dependent maximum in ionic conductivity is essentially independent of concentration and there really appears to be no reason to restrict calculations to low ionic concentrations in computer simulation studies. We have therefore chosen to perform the studies at high concentration. Performing simulations at higher concentrations does not have the disadvantages mentioned earlier.

We now briefly discuss previous investigations into the size-dependent maximum in self-diffusivity observed in a different context. An investigation into the size dependence of self-diffusivity for neutral guest molecules diffusing within porous crystalline solids such as zeolites[39,40] found that with an increase in the size of the guest molecule the self-diffusivity D decreases and has a linear proportionality to the reciprocal of the square of the guest diameter, $D \propto 1/\sigma_{gg}^2$ where σ_{gg} is the size of the guest. This regime is often referred to as the linear regime (LR). Upon further increase in σ_{gg}, D exhibits a maximum. This is the anomalous regime (AR) (see Figure 2). Such a maximum in D is seen when the size of the guest is comparable with that of the void through which it is diffusing. In situations where the void diameter is not uniform, such as in zeolites Y and A, the narrowest part of the void through which the molecule is diffusing, often referred to as the neck or window, is to be considered. Such a maximum owes its origin to the mutual cancellation of the force exerted on the guest by the host. Such a cancellation occurs only when the guest is comparable with the neck diameter and not when the guest and the void diameter are different. This is termed the levitation effect (LE) and has been widely investigated for guests in zeolites and ions in Nasicons.[40−43]

More recently, we have found that such a maximum in self-diffusivity exists even in *liquid mixtures*[43] consisting of a larger component and one or more smaller components. The smaller component is diffusing within the voids defined by the larger component; the difference between this and the zeolite is that here the void network is not only disordered but also evolving in time.[43] Thus, the widely differing conditions under which LE has been seen suggest that it is highly generic in nature and universal. Here, we ask whether it is possible that this maximum seen in simple liquid mixtures also extends to ions in solutions? In fact, we recently proposed that LE could provide an alternative explanation for the maximum in conductivity in water.[44] We also recently reported results to show that even uncharged solutes in water[45] exhibit a maximum in diffusivity albeit at low temperatures. We explore here in more detail the possibility of LE providing a convincing explanation for the observed maximum in the self-diffusion coefficient for ions in water.

Over the past few years, the specific characteristics of the anomalous and the linear regimes of the levitation effect have been studied.[40,41,46] The two regimes have their distinct characteristics and differ in several properties. First, velocity autocorrelation functions for the size corresponding to the maximum in self-diffusivity, exhibits less backscattering, and has little or no foray into the negative regions. In contrast, a particle which is in the linear regime exhibits a pronounced backscattering as seen from the significant negative values of the correlations. Second, the activation energy of the anomalous regime particle is found to be lower than that of the linear regime particle. Third, the intermediate scattering function for the anomalous regime particle exhibits a single-exponential decay. In contrast, the particle in the linear regime exhibits a biexponential decay. Finally, consider $\Delta\omega(k)/2Dk^2$, where $\Delta\omega(k)$ is the full width at half-maximum of the self-part of $S_s(k,\omega)$, the intermediate scattering function at wavevector k, and $2Dk^2$ is the value of $\Delta\omega(k)$ in the limit of $k \rightarrow 0$. This function, $\Delta\omega(k)/2Dk^2$, exhibits a shallow minimum or no pronounced minimum as a function of k. In contrast, a particle from the linear regime exhibits a more pronounced minimum.

Recently, we reported preliminary investigations into the diffusion of ions in water.[44] We examined there the possibility of the levitation effect providing an alternative framework to understand the maximum in diffusivity and conductivity of ions in polar solvents. Here, we report extensive simulations of ions in water at reasonably high concentrations (∼3−4 M) of ions. As mobility and conductivity are related to self-diffusivity, we restrict ourselves to computing the latter. In section 3.1, we present properties of model ions as a function of their size. Structural and diffusion properties of ions in water are presented.

TABLE 1: Water−Water Potential Parameters for the spc/e Model

spc/e	σ_{OO} (Å)	ϵ_{OO} (kJ/mol)	charge (q)
O (H_2O)	3.169	0.6502	−0.8476
H (H_2O)			+0.4238

We also compute the distribution of the void and neck radii present in water through which the ions diffuse. Our results suggest that the diffusion coefficient exhibits a size-dependent maximum for both positively and negatively charged ions. We compute a number of related properties for an ion at the maximum conductivity as well as for an ion far away from maximum conductivity. In section 3.2, we present results for real ions Br^- and Cl^- in water. In section 3.3, we analyze the experimentally measured conductivity data of Kay and Evans[31] for alkali ions in water.

2. Methodology

2.1. Intermolecular Potential. *Water−Water.* We employ the spc/e (*extended simple point charge*) model to simulate water.[47] In this model, water molecule is represented by three sites positioned on the O and H atoms and carrying a similar mass as the respective atoms. The O−H bond length is taken to be 1.0 Å and HOH angle equal to the tetrahedral angle, 109.47°. A charge of $+q$ is placed on H and $-2q$ on O. The short-range interaction is restricted to the oxygen through a Lennard-Jones potential. The pair potential between two water molecules has the form

$$\Phi_{ww} = 4\epsilon_{OO}\left[\left(\frac{\sigma_{OO}}{r_{OO}}\right)^{12} - \left(\frac{\sigma_{OO}}{r_{OO}}\right)^{6}\right] + \sum_{i,j\epsilon w, i\neq j}\frac{q_i q_j}{r_{ij}} \qquad (6)$$

where ϵ_{OO} and σ_{OO} are the Lennard-Jones potential parameters between the oxygen of the two water molecules and r_{OO} is the O−O distance. q_i is the charge at site i. The water−water interaction potential parameters are listed in Table 1.

Solute−Solute. The interaction between two solute molecules is through short-range Lennard-Jones (6-12) and Coulombic potential. The parameters are $\sigma_{ss} = 1.5$ Å and $\epsilon_{ss} = 0.2608$ kJ/mol. The parameter σ_{ss} for solute−solute interaction has not been varied. Thus, the solute−water cross interaction parameters do not obey the Lorentz−Berthelot combination rules. Calculations have been carried out on solute with charges: $q_s = \pm 0.1$, ± 0.3, and ± 0.5 e.

Solute−Water. The solute is represented as a spherical species with a short-range interaction site and a charge. It interacts with water through a short-range interaction with the oxygen of water and Coulombic interaction with charges on the H and O atoms of water.

$$\Phi_{sw} = 4\epsilon_{sO}\left[\left(\frac{\sigma_{sO}}{r_{sO}}\right)^{12} - \left(\frac{\sigma_{sO}}{r_{sO}}\right)^{6}\right] + \sum_{j\epsilon w}\frac{q_s q_j}{r_{sj}} \qquad (7)$$

where ϵ_{sO} and σ_{sO} are the Lennard-Jones potential parameters between solute s and oxygen (O) of the water. q_s is the charge on solute s. r_{sO} and r_{sj} are the solute−oxygen distance and solute−(H,O) distance. Here, solute s is represented by a single site and water by three sites.

We have varied σ_{sO}, the Lennard-Jones parameter, between the solute and the oxygen as well as the charge on the solute, q_s. We keep the interaction strength, ϵ_{sO}, constant at 1.5846 kJ/mol. For $q_s = \pm 0.1$, ± 0.3, and ± 0.5 e, σ_{sO} has been varied between 0.9 and 3.5 Å, 1.0 and 3.5 Å, and 1.1 and 3.5 Å, respectively.

TABLE 2: Halide−Water (spc/e model[47]) Potential Parameters

ion	σ_{sO} (Å)	ϵ_{sO} (kJ/mol)	charge (q)
F^-	3.143	0.6998	−1.0
Br^-	3.854	0.5216	−1.0

Halide Ion−Water Potential Parameters. Calculations have been carried out with a single F^- ion as well as a Br^- ion immersed in water. Hence, solute−solute interaction is absent. These calculations have been carried out as a check of the correctness of our simulation. We used precisely the same parameters as Koneshan et al.[48] (see Table 2). We found our results agree with those of Koneshan et al.

2.2. Voronoi Polyhedra Analysis. We use the Voronoi construction to characterize the structure of the "pore space" or "void space" in water. To characterize the structure of the "void space" in the host matrix, we use the Voronoi construction, which has been employed in similar studies of liquids,[49,50] and other disordered materials such as porous media and powders,[51,52] resulting in valuable insights into the distribution of voids within these dense systems. In any specified configuration of equisized particles, the Voronoi polyhedron of particle i is the set (sub-volume) of all points that are closer to i than to any other. The vertexes and edges of the Voronoi polyhedra are, by construction, equally far from the closest surrounding particles. Specifically, in disordered configurations, a Voronoi vertex is equidistant from four particles, and any point on a Voronoi edge is equidistant from three particles. Therefore, a natural and convenient description of the empty or void space can be given in terms of the network formed by the edges of the Voronoi polyhedra. Specifically, one can visualize the void space as made of "pores", each of radius given by the distance of a Voronoi vertex to the surrounding particles *minus* the particle radius, and "channels" of radius given by the smallest lateral distance of a Voronoi edge and the surrounding particles *minus* the particle radius. We refer to the corresponding diameters as *void* and *neck* radii, respectively. Diffusants of a given radius can find an interconnected path between voids if the intervening neck sizes are larger than the diffusant radius. However, the motion of the host atoms ensures that the void network is restructured dynamically. Thus, even a guest particle for which there is no interconnected path at a given time step manages to diffuse over a period of time.

Voronoi and Delaunay tessellations have been carried out using the algorithm by Tanemura et al.,[53] as outlined in Sastry et al.[50] The main purpose of Voronoi analysis is to obtain the distribution of void and neck diameters. In carrying out the Voronoi analysis, we have made a simplifying assumption that water can be represented as a spherical species. For this, only σ_{OO} (3.169 Å) of the oxygen atom of the water molecule has been utilized for generating the tessellation.[53]

2.3. Molecular Dynamics Simulations. All the simulations have been carried out in the microcanonical ensemble by using the molecular dynamics method. A slightly modified version of DL_POLY program[54] was used. A fifth-order predictor-corrector algorithm has been used to integrate the equations of motion. A cubic periodic boundary condition has been employed throughout the calculation. We use the Ewald sum for the long-range Coulombic interactions. Rotational degrees of freedom have been represented in terms of quaternions.

2.4. Computational Details. *Model Ion.* Four sets of runs in the microcanonical ensemble have been carried out with

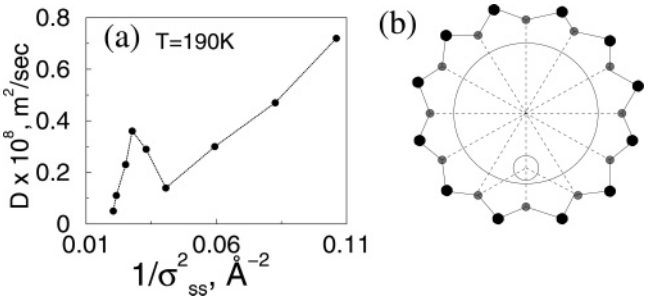

Figure 2. (a) Plot of self-diffusivity vs $1/\sigma_{gg}^2$ in NaY taken from ref 40. (b) Explanation for (a): the bottleneck for diffusion is the 12-membered ring or window in zeolite NaY, shown with Si and O atoms as filled circles. Guest atoms are shown as open circles. For the larger guest with diameter comparable to that of the 12-membered ring, there is a net cancellation of forces while this does not happen for the smaller guest which results in a diffusion maximum when the size of the guest is comparable to the neck diameter.

differing charges placed on the solute ($q_s = \pm 0.1$, ± 0.3, and ± 0.5 e). In each of these four sets, the solute radius σ_{sO} has been varied over a wide range, as suggested by the Voronoi tessellation.

For the ± 0.1, ± 0.3, and ± 0.5 e charged species, we chose 0.6, 0.4, and 0.3 fs, respectively, as the integration time step. The simulation cell is a cube of length 26.0 Å with 466 water molecules corresponding to $\rho = 0.792$ g/cm^3. A cutoff radius of 13.0 Å has been used. We have taken 64 solute particles, consisting of 32 positively and 32 negatively charged solutes. The solute mass is 18 amu, same as the solvent. Calculations have been carried out at 300 K.

Properties have been calculated from configurations stored at intervals of 100 integration steps. The equilibration period is 150 ps during which the velocities are scaled to obtain the desired temperature while the production runs are for 400 ps. Calculation of the void and neck distributions has been carried out with 400 stored configurations.

Br^- and F^- (halide ions). Simulations have been carried out in the NVE ensemble at a density of 0.997 g/cm^3. The simulation cell is a cube of length 24.075 Å with 466 water molecules and one Br^-/F^- ion. The cutoff radius is 12.0 Å. The system as a whole, therefore, has a charge of -1.0 e. In these calculations, the equations of motion of the ion are also integrated. That is, the ions are also permitted to diffuse. Calculations have been carried out at three different temperatures: 258.15, 298.15, and 338.15 K. The integration time step is 1.0 fs. Properties have been computed from configurations stored at an interval of 0.1 ps. Equilibration was performed over a time period of 400 ps, and the production runs were performed over a duration of 600 ps.

3. Results and Discussion

3.1. Size Dependence of Self-diffusivity. In Figure 3, the void ($g(r_v)$) and neck ($g(r_n)$) distributions for $q_s = 0.1$, 0.3, and 0.5 e for three different solute sizes, $\sigma_{sO} = 1.0$, 1.9, and 3.0 Å are shown. From the figure, we can see that, for ions with a charge of 0.5 e, the distribution shows a slight shift toward the larger radius for larger sized solutes. The distribution of the neck radius interconnecting the voids is shown in Figure 3b. The maximum in this also exhibits a slight but noticeable shift to larger values of r_n upon increasing the radius of the ion. For higher sizes of the ion carrying a higher charge, a noticeable broadening in the width of the distribution is also seen.

In Figure 4, we show the time evolution of the mean square displacement for several solute sizes with charge, $q_s = \pm 0.1$ e.

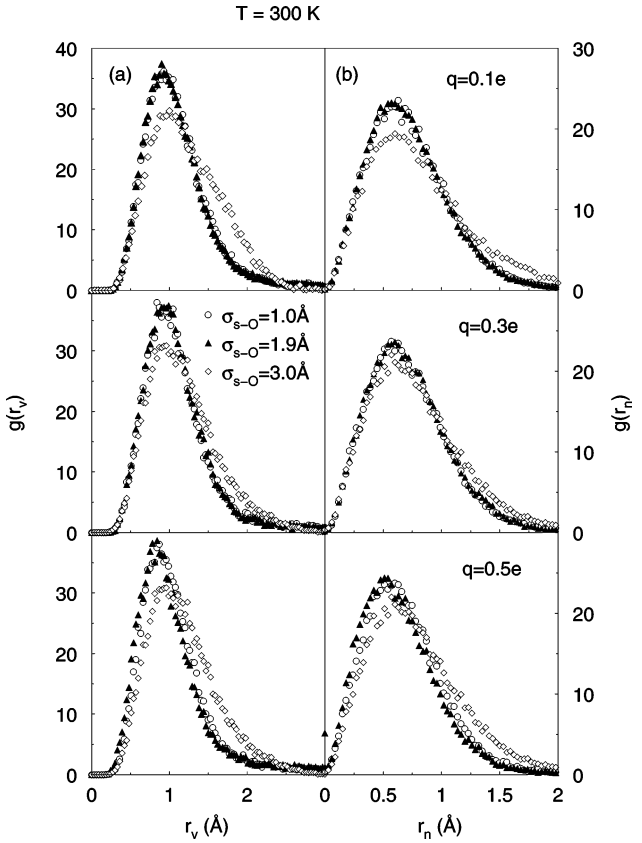

Figure 3. (a) Void and (b) neck distributions of water for positively charged ions for a system with $q_s = \pm 0.1$, ± 0.3, and ± 0.5 e at 300 K in the presence of three different guest ions.

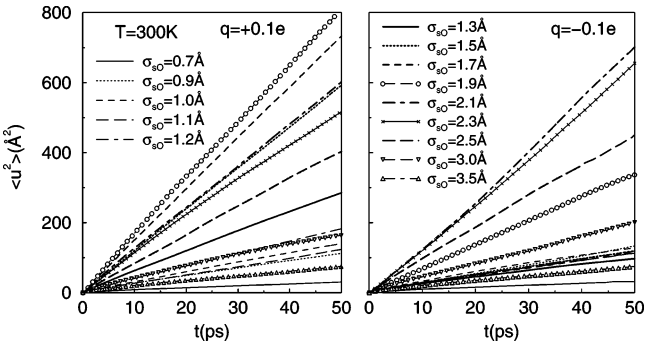

Figure 4. Mean square displacement for $q_s = \pm 0.1$ e at 300 K.

From the slope of msd's, we have calculated the self-diffusivity by using the Einstein relation.[55] The self-diffusivity values are listed in Table 3. Figure 5 shows a plot of self-diffusivity, D, as a function of $1/\sigma_{sO}^2$ for $q_s = \pm 0.1$, ± 0.3, and ± 0.5 e. A diffusion maxima is seen for all of the six cases **irrespective of the magnitude of the charge on the ion**. We note the following trends: (i) A shift of the diffusion maxima toward a larger value of σ_{sO} is observed with an increase in the magnitude of the q_s. (ii) The ratio of D at the maximum to that at the minimum is largest for $q_s = \pm 0.1$ e. A decrease or increase in the magnitude of q_s reduces this ratio. (iii) The diffusion maxima exist even at room temperature ($T = 300$ K).

We note that previously there have been studies of self-diffusivity of ions in water by several groups. Rasaiah, Lynden-Bell, and co-workers have reported diffusivity of alkali and halide ions in water. In these studies, the authors, have varied not only the size (σ_{sO}) but also the mass, interaction strength (ϵ_{sO}), and so forth. They have done so to choose parameters

TABLE 3: Self-Diffusivity Values for $q_s = \pm 0.1$, ± 0.3, and ± 0.5 e at 300 K

	$D \times 10^9$, m^2/s					
σ_{sO} (Å)	$q = 0.1$ e	$q = -0.1$ e	$q = 0.3$ e	$q = -0.3$ e	$q = 0.5$ e	$q = -0.5$ e
0.9	3.58	4.36				
1.0	4.45	3.98	3.01	1.47	2.03	1.56
1.1	4.91	3.53				
1.2	5.93	3.71				
1.3	9.28	2.76	2.67	1.35	1.13	1.08
1.5	19.64	3.58	1.48	1.05	1.00	0.84
1.7	24.91	5.45	2.98	1.32		
1.9	26.77	11.33	4.06	1.42	1.16	0.89
2.1	20.91	23.76	6.11	2.25	1.60	0.95
2.3	17.01	21.51				
2.5	13.45	15.15	3.32	1.79	2.01	1.70
3.0	5.71	6.46	1.91	1.67	2.85	1.30
3.5	2.29	2.01	1.31	1.30	1.5	1.02

that realistically represent the various alkali and halide ions. In one study, they varied the charge on the iodide ion from -1 to 0 to $+1$ to study its effect on self-diffusion. All of these studies were carried out at low molar concentration. Chandra and co-workers[30,56] as well as Bagchi and co-workers[57,58] have also computed the self-diffusivity of ions in water, methanol, and other liquids as well as liquid mixtures. In these studies, Chandra and co-workers[29,59] have attempted to study the hydrogen bond dynamics in the case of water and other properties. Most of these studies are also at a low concentration of ions.

Results obtained here indicate that the diffusivity maximum exists even when the size alone is varied. In other words, size of the ion is responsible for the maximum in diffusivity. Furthermore, we note that such a maximum exists whatever the charge on the solute is. Recently, we have shown that a size-dependent maximum exists for an uncharged solute in water as well, albeit at low temperatures.[45] This result, taken together with results presented here for $q_s = \pm 0.1$, ± 0.3, and ± 0.5 e, suggests that whatever the charge (even $q_s = 0$ e), the size-dependent maximum exists. We have explained elsewhere[45] the reasons for the existence of the maximum at low temperatures for the $q_s = 0$ e case. Thus, it appears that such a maximum is more generic than hitherto believed.

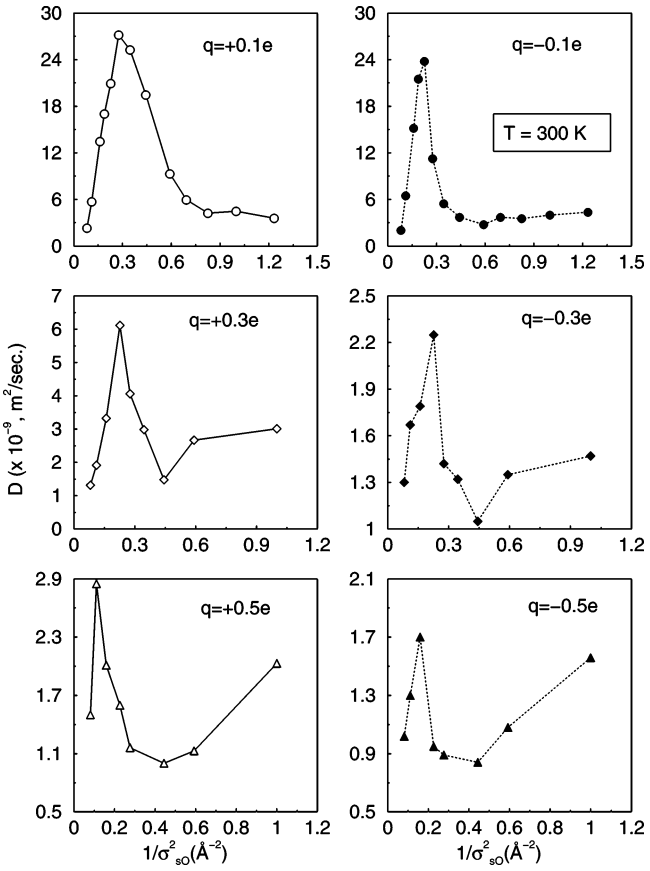

Figure 5. Self-diffusivity, D, as a function of $1/\sigma_{sO}^2$ for $q_s = \pm 0.1$, ± 0.3, and ± 0.5 e at 300 K.

Both the solvent−berg and the continuum theories fail to explain why a diffusivity maximum is seen for an uncharged solute. It is not clear whether microscopic theories in their present form can account for the observed maximum in diffusivity for uncharged solutes.

Recently, we proposed an alternative explanation in terms of the levitation effect for the diffusivity maximum seen for ions in solvents.[44] This can explain, as discussed in the Introduction, the observation of a diffusivity maximum for charged as well as uncharged solutes. We now investigate more thoroughly the appropriateness or validity of the levitation effect to the diffusivity maximum seen here for ions in water by computing a number of other properties and comparing them with the already well-established characteristics of the diffusant from the linear and anomalous regimes discussed in the Introduction. If the computed properties conform to the previously observed properties of LR and AR, then the LE may provide the underlying reason for the diffusivity or conductivity maximum, otherwise referred to as the breakdown of Walden's rule. Note that a similar size-dependent maximum has been seen in guest−zeolite systems or simple liquid mixtures interacting via a Lennard-Jones interaction potential and these have been shown to arise from the LE. Thus, the purpose of the rest of this section is 2-fold: (i) to present a more detailed analysis of the dynamics of ion motion in water and (ii) to investigate to what extent these results agree with the characteristics of the LR and AR of the levitation effect.

In Figure 6, we show the velocity correlation functions (vacf's) for various sizes of the ion at 300 K for $q =$ (a) 0.1 e, (b) -0.1 e, (c) 0.3 e, and (d) 0.5 e, respectively. Note that vacf's show shallow minima and less undulations corresponding to maxima in D for all the charges. The curves exhibit significant negative correlations for all values of σ_{sO} except the value of σ_{sO} where the maximum in D is observed. This suggests that the potential energy (p.e.) landscape is rather flat for σ_{sO} values corresponding to the maximum in D. This may be compared with the earlier studies of quite different systems. Previous studies on monatomic sorbates in zeolites[60] have shown that, for particles in the anomalous regime, the p.e. surface is relatively flat in comparison with those in the linear regime. The vacf obtained here confirms that the p.e. surface is flat for the anomalous regime even among the ions diffusing in water. The study on the binary mixture interacting via a simple (6-12)

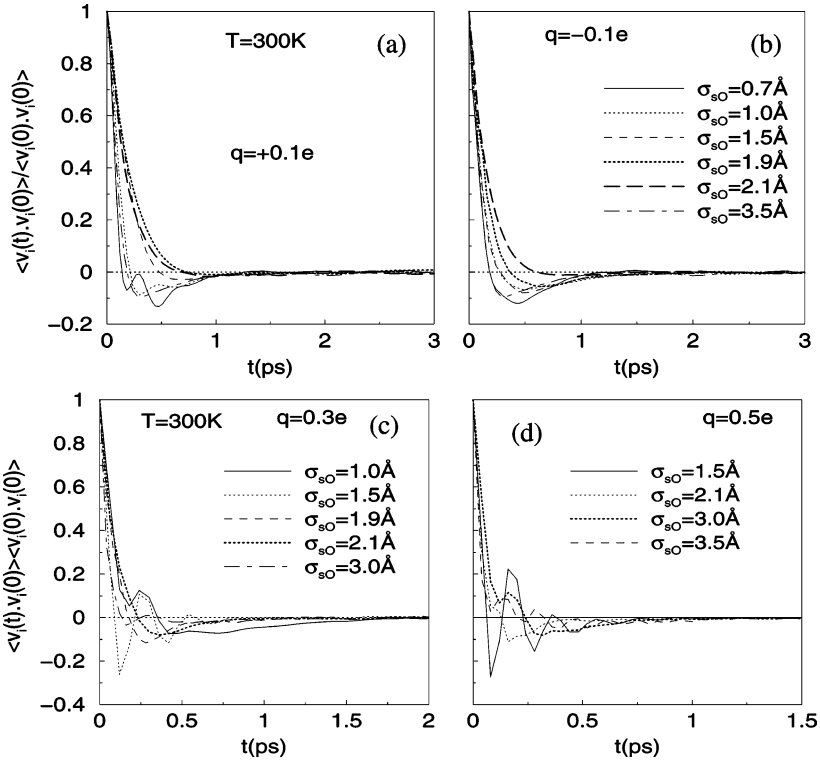

Figure 6. Velocity autocorrelation function (vacf) for the ions at a few selected sizes for $q_s = \pm 0.1$ and 0.3 and 0.5 e at 300 K.

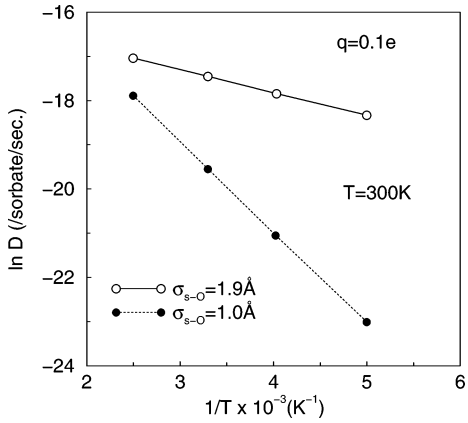

Figure 7. Arrhenius plot of the self-diffusivity D for the positively charged ion for a system with $q = \pm 0.1$ e.

TABLE 4: Self-Diffusivity Values for the Positively Charged Ion in the Linear ($\sigma_{sO} = 1.0$ Å) and Anomalous ($\sigma_{sO} = 1.9$ Å) Regimes at Various Temperatures for a System Consisting of Solutes with $q = \pm 0.1$ e

σ_{sO} (Å)	$D_{200K} \times 10^8$ (m^2/s)	$D_{250K} \times 10^8$ (m^2/s)	$D_{300K} \times 10^8$ (m^2/s)	$D_{400K} \times 10^8$ (m^2/s)
1.0 (LR)	0.0098	0.069	0.45	1.60
1.9 (AR)	1.01	1.72	2.67	3.91

Lennard-Jones potential also showed that the p.e. landscape for the particle with maximum self-diffusivity has only small undulations.[43]

An Arrhenius plot of ln D vs $1/T$ is shown in Figure 7 for $q = 0.1$ e. The self-diffusivity, D, has been calculated for four different temperatures. The values of D are listed in Table 4 for two sizes of the ion, $\sigma_{sO} = 1.0$ and 1.9 Å. From the figure, it is evident that the slope of $\sigma_{sO} = 1.0$ Å is significantly higher than that of $\sigma_{sO} = 1.9$ Å. The activation energies (E_a) are 17.26 and 4.31 kJ/mol for the ion in linear ($\sigma_{sO} = 1.0$ Å) and anomalous ($\sigma_{sO} = 1.9$ Å) regimes, respectively. This significant lowering of activation energy suggested by the LE for a particle near the diffusivity maximum seems to be valid for ions in water. A comparison with previously reported activation energies suggests that the difference between the values of activation energy for linear and anomalous regimes is usually 2−3 kJ/mol. In the present study, this difference between the activation energies for the ion at the maximum and in the linear regime is significant. We shall discuss this aspect as well as the implications it has for various theories or models in more detail later. Here, it suffices to note that the observed trend is in conformity with the predictions of the LE.

The intermediate scattering function, $F_s(k,t)$, is shown in Figure 8 and Figure 9 for ions from linear and anomalous regimes, respectively, for $k = 0.96$ Å^{-1} at 300 K for $q_s = 0.1$, 0.3, and 0.5 e. We have calculated $F_s(k,t)$ for two different sizes, one corresponding to the size close to diffusion maximum and another at a size close to diffusion minimum. We have also shown the single (e^{-t/τ_1}) and biexponential ($e^{-t/\tau_1} + e^{-t/\tau_2}$) fits to the smaller sized ion and the single-exponential (e^{-t/τ_1}) fit for the ion in the anomalous regime. A single-exponential decay provides a good fit to the $F_s(k,t)$ for the particle in the anomalous regime (see Figure 9) but not to the particle in the linear regime (see Figure 8). Explanations for these are similar to those we provided for the case of uncharged solute. There are, however, differences between the results for the uncharged solute and ions which we shall discuss elsewhere.

Variations of $\Delta\omega(k)/2Dk^2$ for two different sizes which exhibit maximum and minimum in self-diffusivity are shown in Figure 10 at 300 K for $q_s = +0.1$, $+0.3$, and $+0.5$ e. The variation of $\Delta\omega(k)/2Dk^2$ with k is large (shows deep minimum) for the ion corresponding to diffusion minimum (LR). In contrast, the variation is relatively smooth over a much smaller range for the size corresponding to diffusion maximum (AR). In other words, no significant slow down is seen for an ion from AR

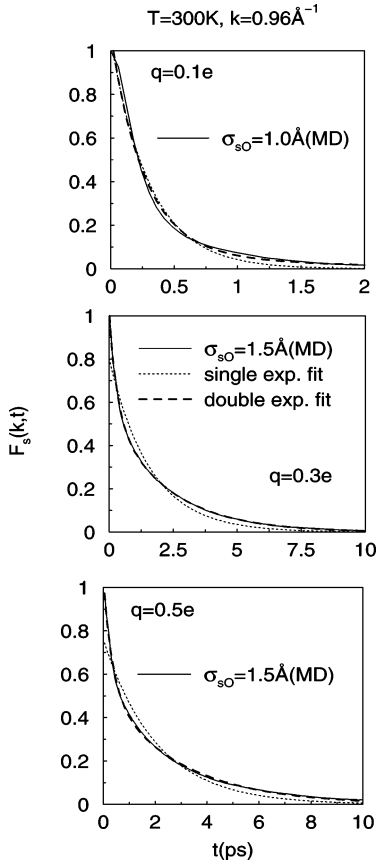

Figure 8. Intermediate scattering function, $F_s(k,t)$, for the ions in the linear regime is shown along with single (e^{-t/τ_1}) and biexponential ($e^{-t/\tau_1} + e^{-t/\tau_2}$) fits for the positively charged ions for $q_s = \pm 0.1$, ± 0.3, and ± 0.5 e at 300 K.

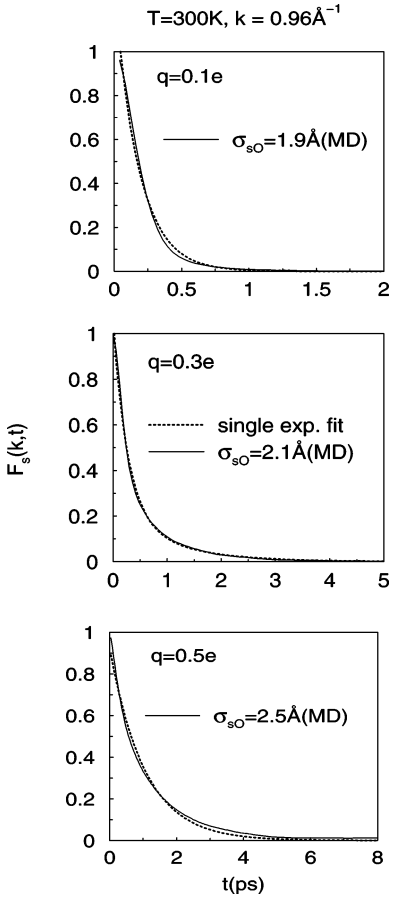

Figure 9. Intermediate scattering function, $F_s(k,t)$, for the ions in the anomalous regime is shown along with the single-exponential (e^{-t/τ_1}) fit for the positively charged ions for $q_s = \pm 0.1$, ± 0.3, and ± 0.5 e at 300 K.

but for an ion from LR a significant slow down is seen at intermediate k values.

Now we discuss a few other relevant properties. In Figure 11, we report the force−force autocorrelation function (facf) for two different sized ions, one from the linear regime (σ_{sO} = 1.5 Å) and another from the anomalous regime (σ_{sO} = 2.1 Å), for $q = 0.3$ and 0.5 e at 300 K. Here, force refers to the total force exerted on the ion by the other ions as well as the solvent (water). A smooth decay is seen for the size corresponding to the diffusion maximum (σ_{sO} = 2.1 Å) while large oscillations are seen for the size which lies at the minimum in the D vs $1/\sigma^2$ plot (see Figure 5). Oscillations are due to the relatively lower mass of the ion in comparison with the solvent.

Diffusivity Maximum for Uncharged and Charge Solutes and the Role of Interactions. As demonstrated previously,[40] the interactions between the diffusant and the medium through which it is diffusing play an important role in giving rise to the diffusivity maximum. It has been found that, in systems interacting with purely short-range interactions, the presence of dispersion interactions is essential for the existence of a size-dependent diffusivity maximum. In such systems, there is a change in activation energy on going from the LR to AR. It is seen that the activation energies of the AR are lower by a few, typically 1−4 kJ/mol, at best. Here, we see a significantly larger change in the activation energies (on the order of 12−13 kJ/mol). This large difference in the activation energy between the LR and AR in the presence of electrostatic interactions needs to be accounted for. Previously, we have shown that the stronger the interaction between the diffusant and its medium through which it is diffusing (in comparison with the kinetic energy), the more significant is the height of the diffusivity maximum. Furthermore, the change in activation energy between the LR and AR is also large when the interactions between the diffusant and the medium are large. The presence of electrostatic interactions between the ion and the medium (water) significantly increases the total interaction energy. As a consequence, the changes in activation energy are large. Furthermore, we can explain the changes in diffusivity observed for the uncharged solute (at 30 K) based on the interactions between the solute and water. The absence of electrostatic or polarization interactions in this case leads to a relatively smaller interaction energy between the solute and the medium, water. As a result, the diffusivity maximum is seen only when the kinetic energy is lower than this interaction energy. As a result, the diffusivity maximum is not seen at high temperatures where the kinetic energy exceeds the weak dispersion forces. Thus, at room temperature, no diffusivity maximum is seen for an uncharged solute. Only at low temperatures can a maximum be seen in the case of uncharged solute. However, as soon as electrostatic or polarization interactions are present (which is present over an extended distance beyond the first two shells of the solvent; this increases the overall interaction strength between the ion and water), the maximum is seen even at room temperature. Thus, the present study in combination with the previous study[61] predicts that there is a maximum in self-diffusivity for uncharged solute provided these measurements are made at rather low temperatures. However, note that the self-diffusivities are low at these low temperatures and therefore measurement of D may be difficult. Thus, the diffusivity or conductivity maximum is

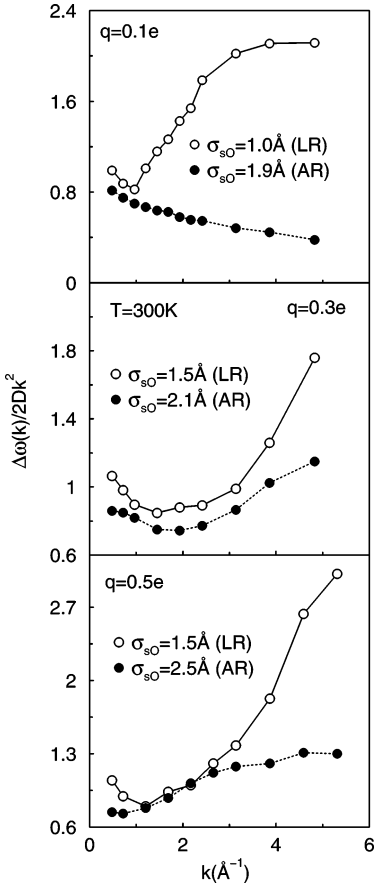

Figure 10. $\Delta\omega(k)/2Dk^2$ as a function of k for the positively charged ions for $q_s = \pm 0.1$, ± 0.3, and ± 0.5 e at 300 K.

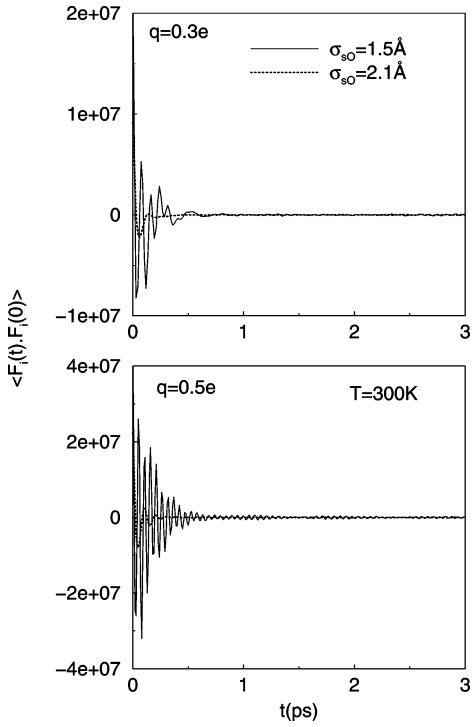

Figure 11. Force autocorrelation function for the positively charged ions in the linear ($\sigma_{sO} = 1.5$ Å) and anomalous ($\sigma_{sO} = 2.1$ Å) regimes at 300 K for a system consisting of solutes with $q_s = \pm 0.3$ and ± 0.5 e. Large oscillations for the smaller ion are due to the relatively lower mass employed in this study.

seen whenever dispersion with or without electrostatic or polarization interactions are present.

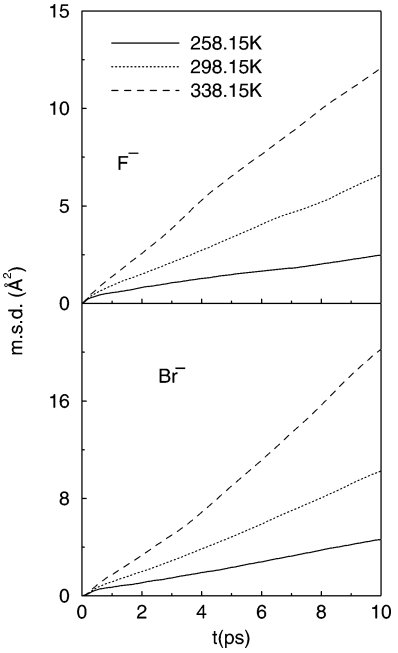

Figure 12. Mean square displacement for F^- and Br^- at three different temperatures.

As the calculations are on model ions here, it is difficult to compare our results with those of actual alkali and halide ions diffusing within water. How far are these observations of the characteristics (such as lowered activation energy, single and biexponential decay of $F_s(k,t)$, etc.) of the LR and AR seen by us here applicable to realistic ions in water? To answer this question, we have carried out calculations on ions using realistic interaction potentials and correct masses. We present the results of these studies below.

3.2. Real Solutes: F^- and Br^- in Water. Experimentally both positively and negatively charged ions in water exhibit a maximum in limiting ion conductivity. This has been previously investigated by simulations[48] and experiments,[31] and they find Br^- in water at 25° C has a higher mobility than F^-. We have carried out simulations of a single ion of F^- and Br^- in water for a density of 0.997 g/cm^3 at three different temperatures (258.15, 298.15, and 338.15 K). We choose a single ion as Koneshan et al. also used a single ion,[48] to enable comparison with experiments. The purpose of these calculations is to carry out a simulation on a realistic system for which the experiment can be performed or has already been performed. But we also compute other properties such as activation energy or $\Delta\omega(k)/2Dk^2$ to see if the ion at the maximum has characteristics that are similar to the AR and the ion at the minimum has characteristics that are similar to a particle from the LR. This will indicate whether the difference in ionic conductivity in this realistic system can be attributed to the levitation effect.

Figure 12 shows the time evolution of the mean square displacement (msd) for F^- and Br^- at 258.15, 278.15, 298.15, and 338.15 K. From the slope of the msd plot, we have calculated the self-diffusivity, D, of F^- and Br^- by using the Einstein relation.[55] The values of D are listed in Table 5. At all the temperatures, the diffusivity of Br^- is larger when compared to F^-. From the previous discussion, it is evident that F^- belongs to the LR and Br^- to the AR of the LE.

The activation energy of the diffusants in the LR has been previously found to be higher than those in the AR. Figure 13 shows the Arrhenius plot of self-diffusivity, D, along with a straight line fit to the data points. From the slope of the least-

TABLE 5: Diffusivity of F^- and Br^- at Four Different Temperatures

	$D \times 10^8$, m^2/s			
ion	$T = 258.15$ K	$T = 278.15$ K	$T = 298.15$ K	$T = 338.15$ K
F^-	0.035	0.061	0.105	0.202
Br^-	0.074	0.112	0.175	0.291

squares fit line, we found the activation energy, E_a, to be 15.96 kJ/mol for F^- and 12.34 kJ/mol for Br^-. This clearly shows that the activation energy is lower for the particle in the AR (Br^-). These are in agreement with previous results on guests in porous solids such as zeolite NaY, NaCaA, and so forth,[62] and in dense fluids.[43]

We have calculated the intermediate scattering function for Br^- and F^- for two different k values, $k = 0.78$ and 1.04 Å^{-1} at 258.15 K (see Figure 14). To the $F_s(k,t)$, we have fitted single (e^{-t/τ_1}) (for Br^- which is in the AR) and double exponential ($e^{-t/\tau_1} + e^{-t/\tau_2}$) (for F^- which is in the LR) for different k values. The values of τ_1 for Br^- (AR ion) and τ_1 and τ_2 for F^- (LR ion) are listed in Table 6. A single-exponential decay provides a good fit to the $F_s(k,t)$ for the Br^- ion but not to the F^- ion (see Figure 14). For the F^- ion, a double exponential provides a good fit.

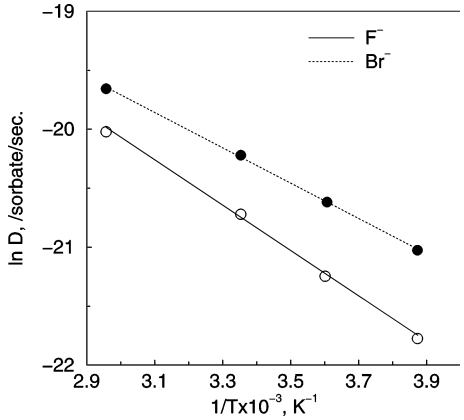

Figure 13. Arrhenius plot of the self-diffusivity D for Br^- and F^-. MD calculations are on a single ion in water.

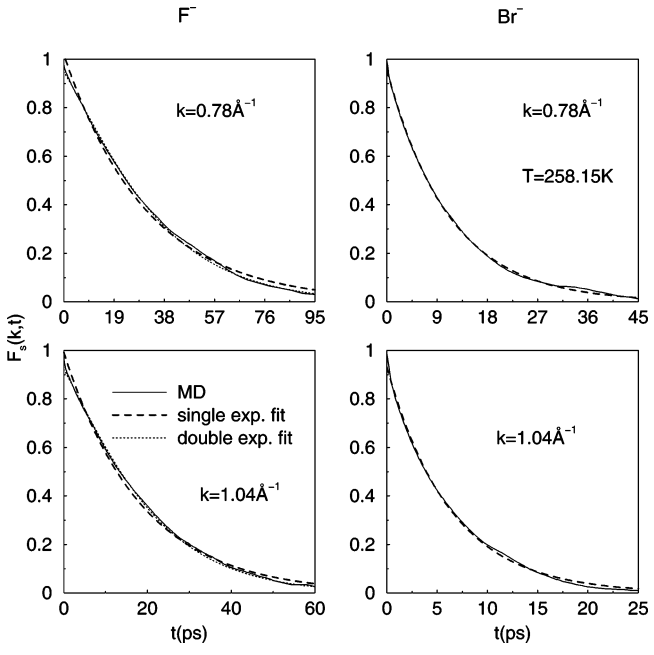

Figure 14. Intermediate scattering function, $F_s(k,t)$, for Br^- and F^-.

TABLE 6: Values of τ_1 for Br^- (AR ion) and τ_1 and τ_2 for F^- (LR ion) for $k = 0.78$ and 1.04 Å^{-1} at 300 K

F^-				Br^-	
$k = 0.78$ Å^{-1}		$k = 1.04$ Å^{-1}		$k = 0.78$ Å^{-1}	$k = 1.04$ Å^{-1}
τ_1 (ps)	τ_2 (ps)	τ_1 (ps)	τ_2 (ps)	τ_1 (ps)	τ_1 (ps)
35.7	33.3	19.6	18.2	11.2	6.3

We now investigate the dependence of the diffusion properties on wavenumber, k, for intermediate k values. We have computed the $\Delta\omega(k)$ in the intermediate k region for a F^- ion and Br^- ion at 258.15 K. As already mentioned, the full width at half-maximum of the self-part of $S_s(k,\omega)$ provides an estimate of the magnitude of the self-diffusivity, $\Delta\omega(k) \propto D(k)$. Figure 15 shows the variation of $\Delta\omega(k)/2Dk^2$ as a function of k. It is seen that for the F^- ion there is a deep minimum. For the Br^- ion, a shallow minimum is observed. The minimum in $\Delta\omega(k)/2Dk^2$ for F^- (LR ion) seen could arise from the energetic barrier for getting past the shells of neighbors, probably the first shell of neighbors. For Br^- (AR ion), the shallow minimum is seen probably due to the presence of a lower energetic barrier. Thus, the motion in the intermediate range of k values is strongly influenced by the intermolecular potential.

We calculate the friction coefficients (ζ) for F^- and Br^- from the force−force autocorrelation function at 298.15 K. They are 2.55×10^{-12} kg/s for F^- and 0.34×10^{-12} kg/s for Br^-. The friction on Br^- (AR ion) is less as compared with that on F^- (LR ion).

The solvent−berg model proposed first to explain the conductivity maximum, and the subsequently proposed continuum models do capture some of the features of the observed maximum. The recent microscopic theories discussed earlier also provide a more detailed picture and are able to reproduce more closely the conductivity variation with size. However, there are still many experimental measurements and trends in the literature. For example, the experimental measurements of Kay and Evans as well as Ueno and co-workers have shown that the Na^+ conductivity in water initially increases with pressure at room temperature and decreases subsequently upon further increase in pressure.[31,33] It is not at all clear that any of the existing models can account for these observed trends. We believe that the levitation effect provides the correct explanation for the observed maximum in conductivity. The effect is highly generic and universal and applies to diverse systems such as guest diffusion in porous solids such as zeolites, diffusion within dense liquids, or ion conductivity in polar solvents. We shall discuss in future communications how the levitation effect

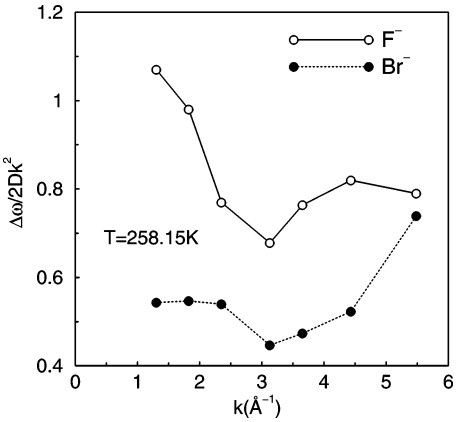

Figure 15. Variation of $\Delta\omega(k)/2Dk^2$ as a function of k for F^- and Br^- at 258.15 K.

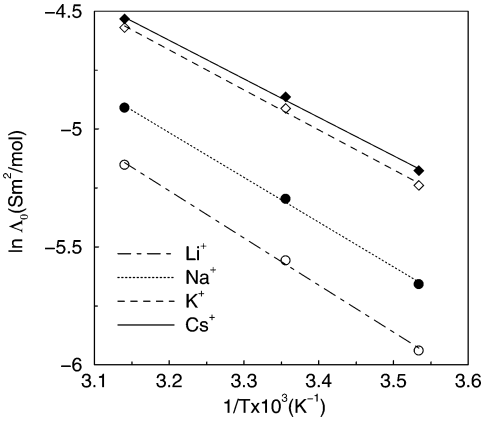

Figure 16. Arrhenius plot of the logarithm of limiting ion conductivity against reciprocal temperature for different alkali ions. The experimental values of conductivity have been taken from Kay and Evans.[31]

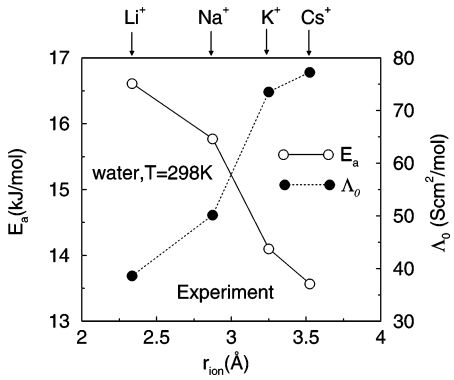

Figure 17. Dependence of activation energy for different alkali ions, obtained from the experimental measurements of ionic conductivity at several temperatures by Kay and Evans.[31] The trend in activation energy is in agreement with the prediction of the LE.

accounts for several of the existing experimental observations in the literature.

We have seen that even simulations of real ions exhibit behaviors in several properties which conforms to the predictions of the LE.

3.3. Experimental Conductivity Data and the LE. We now analyze existing experimental data in the literature. We have seen that one of the predictions of the LE is that the activation energy is lower for the ion size corresponding to the maximum in self-diffusivity. Is this found experimentally? We look at the available experimental data in the literature.

We plot in Figure 16 the logarithm of ionic conductivity against reciprocal temperature for four ions in water. The data have been taken from Kay and Evans.[31] The resulting activation energies are plotted in Figure 17. The activation energy shows a decrease from around 16.6 kJ/mol for Li^+ to around 13.6 kJ/mol for Cs^+. The conductivities at room temperature are also shown in the figure. We note that none of the existing theories, to the best of our knowledge, predict a lower activation energy for the ion with maximum conductivity. A lower activation energy is, however, predicted by the LE. Thus, this experimental observation of lower E_a for the ion with maximum diffusivity is in agreement with the LE.

4. Conclusions

The simulations on model ions have been carried out at high concentrations (∼3 M). The results suggest for the first time that the size-dependent diffusivity maximum persists up to high loadings. This is in agreement with the experimental measurements of Goldsack et al.[38] who found that, at least up to a concentration of 9 M, the size-dependent maximum persists. We note that all previous studies have been carried out at dilute concentrations (∼0.1 M).

We have computed void and neck distributions, self-diffusivity, E_a, $F_s(k,t)$ for small k values, $\Delta\omega(k)/2Dk^2$, and so forth, which have been reported for different sizes and charges of the ion ($q_s = \pm 0.1$, ± 0.3, and ± 0.5 e). This along with the previous result of ours on uncharged solute show that the diffusivity maximum exists irrespective of the charge on the ion. The computed properties show trends similar to that observed for the linear and anomalous regimes of the LE depending on the radius of the ion. These provide further evidence that the diffusivity maximum may have its origin in the levitation effect.

As far as we know, there have not been any previous studies which have recognized or even remotely suggested a lower activation energy for the ion with maximum conductivity. Our simulations of real ions F^- and Cl^- and the experimental conductivity data confirm a lower activation energy for the AR again consistent with the LE. This is the first time that a lower activation energy for the ion with maximum conductivity has been noted. To the best of our knowledge, none of the existing theories predict a lower activation energy for the ion with a maximum conductivity with the exception of the LE.

The present study suggests that the uncharged solute and the charged solute are treated in a similar fashion within the LE. There are no significant differences between them in terms of the existence of the diffusivity maximum. However, the nature of the electrostatic interactions do make a significant difference in several ways. First, the presence of electrostatic interactions increase the solute−solvent interaction significantly and therefore lead to the presence of a diffusivity maximum at room or still higher temperatures. Second, they lead to a significant difference in activation energies between the ion at the diffusivity maximum and away from the maximum. Since the Coulombic interactions are long-ranged, the smallest amount of charge on the solute acts as a step function; even though charges on the solute are weak, the sum over several shells of the solvent adds up to a significant interaction energy. This explains why no one has so far found uncharged solutes exhibiting a diffusivity maximum; they exist only at low temperatures, where most solvents cease to be liquids.

The existing theories have successfully explained the conductivity variation with size, but there are a number of other experimental data that remain to be accounted for (see, for example, the works of Kay and co-workers[31,63] and Ueno and co-workers[32,33,64,65]).

The proposed explanation in terms of the LE provide a unified and generic explanation for the existence of a diffusivity maximum not only in simple liquid mixtures interacting via van der Waals interaction and ion conductivity in polar solvent but also for guest molecules diffusing in porous solids such as zeolite. Such a unified explanation has implications in diverse areas such as condensed matter, physical chemistry, and material science. They are also likely to be important in biological systems.

Acknowledgment. We wish to thank the Department of Science and Technology, New Delhi, for financial support. The authors acknowledge Professor Masakatsu Ueno for his effort and timely help in bringing to our attention the reference of Goldsack et al.[38] on the conductivity measurements at high ionic concentrations as a function of the size of the ion.

References and Notes

(1) Falkenhagen, H. *Electrolytes*; Clarendon Press: Oxford, U.K., 1934.
(2) Atkins, P. W. *Physical Chemistry*; Oxford University Press: Oxford, U.K., 1994.
(3) Glasstone, S. *An Introduction to Electrochemistry*; Litton Education Publishing: New York, 1971.
(4) Castellan, G. W. *Physical Chemistry*; Addition-Wesley, Reading, MA, 1971.
(5) Bagchi, B.; Biswas, R. *Acc. Chem. Res.* **1998**, *31*, 181.
(6) Born, M. *Z. Phys.* **1920**, *1*, 221.
(7) Chen, J. H.; Adelman, S. A. *J. Chem. Phys.* **1980**, *72*, 2819.
(8) Fuoss, R. M. *Proc. Natl. Acad. Sci.* **1959**, *45*, 807.
(9) Boyd, R. H. *J. Chem. Phys.* **1961**, *35*, 1281.
(10) Zwanzig, R. *J. Chem. Phys.* **1970**, *52*, 3625.
(11) Hubbard, J. B.; Onsager, L. *J. Chem. Phys.* **1977**, *67*, 4850.
(12) Zwanzig, R. *J. Chem. Phys.* **1963**, *38*, 1603.
(13) Koneshan, S.; Lynden-Bell, R. M.; Rasaiah, J. C. *J. Am. Chem. Soc.* **1998**, *120*, 12041.
(14) Bagchi, B. *J. Chem. Phys.* **1991**, *95*, 467.
(15) Biswas, R.; Roy, S.; Bagchi, B. *Phys. Rev. Lett.* **1995**, *75*, 1098.
(16) Biswas, R.; Bagchi, B. *J. Chem. Phys.* **1997**, *106*, 5587.
(17) Biswas, R.; Bagchi, B. *J. Am. Chem. Soc.* **1997**, *119*, 5946.
(18) Roy, S.; Bagchi, B. *J. Chem. Phys.* **1993**, *99*, 9938.
(19) Roy, S.; Bagchi, B. *J. Chem. Phys.* **1994**, *101*, 4150.
(20) Nandi, N.; Roy, S.; Bagchi, B. *J. Chem. Phys.* **1995**, *102*, 1390.
(21) Biswas, R.; Nandi, N.; Bagchi, B. *J. Phys. Chem.* **1997**, *101*, 2698.
(22) Bhattacharya, S.; Bagchi, B. *J. Chem. Phys.* **1997**, *106*, 1757.
(23) Maroncelli, M.; Fleming, G. *J. Chem. Phys.* **1988**, *89*, 5044.
(24) Barbara, P. F.; Jarzeba, W. *Adv. Photochem.* **1990**, *15*, 1.
(25) Bagchi, B. *Annu. Rev. Phys. Chem.* **1989**, *40*, 115.
(26) Lee, S. H.; Rasaiah, J. C. *J. Chem. Phys.* **1994**, *101*, 6964.
(27) Lynden-Bell, R. M.; Kosloff, R.; Ruhman, S.; Danovich, D.; Vala, J. *J. Chem. Phys.* **1998**, *109*, 9928.
(28) Chandra, A. *Phys. Rev. Lett.* **2000**, *85*, 768.
(29) Chandra, A.; Chowdhury, S. *Proc.−Indian Acad. Sci., Chem. Sci.* **2001**, *113*, 591.
(30) Chandra, S. C. A. *J. Chem. Phys.* **2001**, *115*, 3732.
(31) Kay, R.; Evans, D. F. *J. Phys. Chem.* **1966**, *70*, 2325.
(32) Ueno, M.; Ito, K.; Tsuchihashi, N.; Shimizu, K. *Bull. Chem. Soc. Jpn.* **1986**, *59*, 1175.
(33) Ueno, M.; Tsuchihashi, N.; Yoshida, K.; Ibuki, K. *J. Chem. Phys.* **1996**, *105*, 3662.
(34) Ibuki, K.; Ueno, M.; Nakahara, M. *J. Mol. Liq.* **2002**, *98−99*, 129.
(35) Hoshina, T.; Tsuchihashi, N.; Ibuki, K.; Ueno, M. *J. Chem. Phys.* **2004**, *120*, 4355.
(36) Thomas, J.; Evans, D. F. *J. Phys. Chem.* **1970**, *74*, 3812.
(37) Horng, M. L.; Gardecki, J. A.; Papazyan, A.; Maroncelli, M. *J. Phys. Chem.* **1995**, *99*, 17311.
(38) Goldsack, D.; Franchetto, R.; Franchetto, A. *Can. J. Chem.* **1976**, *54*, 2953.
(39) Yashonath, S.; Santikary, P. *J. Chem. Phys.* **1994**, *100*, 4013.
(40) Yashonath, S.; Santikary, P. *J. Phys. Chem.* **1994**, *98*, 6368.
(41) Yashonath, S.; Rajappa, C. *Faraday Discuss.* **1997**, *106*, 105.
(42) Padmanabhan, P. K.; Yashonath, S. *J. Phys. Chem.* **2002**, *106*, 3443.
(43) Ghorai, P. K.; Yashonath, S. *J. Phys. Chem. B* **2005**, *109*, 5824.
(44) Ghorai, P. K.; Yashonath, S.; Bell, R. L. *J. Phys. Chem. B* **2005**, *109*, 8120.
(45) Ghorai, P. K.; Yashonath, S. Submitted for publication, 2006.
(46) Ghorai, P. K.; Yashonath, S. *J. Phys. Chem. B* **2005**, *109*, 3979.
(47) Berendsen, H. J. C.; Grigera, J. R.; Straatsma, T. P. *J. Phys. Chem.* **1987**, *91*, 6269.
(48) Koneshan, S.; Rasaiah, J. C.; Lynden-Bell, R. M.; Lee, S. H. *J. Phys. Chem. B* **1998**, *102*, 4193.
(49) Corti, D. S.; Debenedetti, P. G.; Sastry, S.; Stillinger, F. H. *Phys. Rev. E* **1997**, *55*, 5522.
(50) Sastry, S.; Corti, D. S.; Debenedetti, P. G.; Stillinger, F. H. *Phys. Rev. E* **1997**, *56*, 5524.
(51) Weissberg, H. L.; Prager, S. *Phys. Fluids* **1962**, *5*, 1390.
(52) Shahinpoor, M. *Powder Technol.* **1980**, *25*, 163.
(53) Tanemura, M.; Ogawa, T.; Ogita, N. *J. Comput. Phys.* **1983**, *51*, 191.
(54) Forester, T. R.; Smith, W. *The DL-POLY-2.0 Reference Manual*, version 2.0; CCLRC, Daresbury Laboratory: Warrington, U.K, 1985.
(55) Allen, M. P.; Tildesley, D. J. *Computer Simulation of Liquids*; Clarendon Press: Oxford, U.K., 1987.
(56) Chowdhury, S.; Chandra, A. *J. Chem. Phys.* **2003**, *119*, 4360.
(57) Biswas, R.; Nandi, N.; Bagchi, B. *J. Phys. Chem.* **1997**, *101*, 2968.
(58) Bagchi, B. *J. Chem. Phys.* **1994**, *100*, 6658.
(59) Chowdhury, S.; Chandra, A. *Phys. Rev. E* **2002**, *66*, 041203.
(60) Rajappa, C.; Yashonath, S. *J. Chem. Phys.* **1999**, *110*, 1.
(61) Ghorai, P. K.; Yashonath, S. *J. Phys. Chem. B* **2004**, *108*, 7098.
(62) Rajappa, C.; Yashonath, S. *Mol. Phys.* **2000**, *98*, 657.
(63) Kay, R. L.; Evans, D. F. *J. Phys. Chem.* **1965**, *70*, 4216.
(64) Nakahara, M.; Zenke, M.; Ueno, M.; Shimizu, K. *J. Chem. Phys.* **1985**, *83*, 280.
(65) Yoshida, K.; Ibuki, K.; Ueno, M. *J. Chem. Phys.* **1998**, *108*, 1360.